

Modelling evolution in the near field of a cementitious repository

A. R. HOCH^{1,*}, G. M. N. BASTON¹, F. P. GLASSER², F. M. I. HUNTER¹ AND V. SMITH¹

¹ AMEC, Harwell Science and Innovation Campus, Harwell, Didcot, Oxfordshire OX11 0QB, UK

² Department of Chemistry, School of Natural and Computing Sciences, University of Aberdeen, Meston Building, Meston Walk, Aberdeen AB24 3UE, UK

[Received 8 January 2012; Accepted 19 November 2012; Associate Editor: Nicholas Evans]

ABSTRACT

In the United Kingdom, disposal of radioactive waste may involve packages of grouted waste being placed in a geological disposal facility (GDF) and surrounded by a cementitious backfill. This paper describes modelling that has been carried out to develop an understanding of the possible spatial and temporal evolution within the GDF.

A single waste package is assumed to be filled with an encapsulation grout, placed in an underground vault and surrounded by a cementitious backfill. Groundwater from the host rock flows into the vault and through the backfill. A simplified model system examines the interactions between groundwater, cementitious backfill and grout.

In most cases the model predicts a reduction in the backfill porosity due to precipitation and dissolution reactions, particularly at the upstream edge of the vault. The degree to which this occurs depends on the groundwater composition. The model also predicts precipitation and dissolution reactions would occur in the grouts close to their interface with the backfill, reducing the local porosity significantly which may isolate the grouts from the backfill, so that the pH within the grouts would be unchanged over an extended period.

KEYWORDS: transport modelling, *TOUGHREACT*, cement, geological disposal facility, radioactive waste.

Introduction

In the United Kingdom, one possible concept for disposing of intermediate- and certain low-level radioactive wastes envisages that packages of waste will be placed in the vaults of a geological disposal facility (GDF), and then surrounded by a cementitious backfill (Nuclear Decommissioning Authority, 2010a). The wastes may be encapsulated or immobilized in a solid matrix, or may be emplaced in containers without encapsulant. A number of waste encapsulation grouts have been developed (Nuclear Decommissioning Authority, 2010b). The cementitious backfill is part of an engineered multi-barrier concept to limit the

migration of radionuclides from a GDF. A formulations for a possible UK backfill, the Nirex reference vault backfill (NRVB) has been developed (Francis *et al.*, 1997; Nuclear Decommissioning Authority, 2010b). The NRVB is designed to provide the alkaline conditions and sorption capacity that are the principal features of chemical conditioning in a GDF, and thereby the provision of a chemical barrier to radionuclide migration from the near field. The NRVB will be required to maintain a high pH environment (pH >10 for at least one million years, Nuclear Decommissioning Authority, 2010a) a large surface area for sorption and a relatively high permeability and porosity (Nuclear Decommissioning Authority, 2010b).

The near field is defined as the engineered multi-barrier system and those parts of the surrounding host rock whose characteristics have

* E-mail: andrew.hoch@amec.com
DOI: 10.1180/minmag.2012.076.8.21

been or could be altered by the GDF or its contents (Nuclear Decommissioning Authority, 2010b). The physical and chemical properties of the near field will evolve as groundwater percolates through the GDF and chemical reactions occur. It is important to understand these processes as part of determining the expected long-term effectiveness of the near field in limiting radionuclide migration.

Expected evolution of pH in the backfill

The hydrated backfill will contain a number of minerals, with the exact mineral assemblage dependant on the formulation, curing time and temperature. The evolution of cement-based backfill in the near field of a GDF will be driven by a number of processes that may occur under post-closure conditions. Initially, the main components are expected to be alkali (i.e. Na, K) hydroxides/sulfates; portlandite, $\text{Ca}(\text{OH})_2$; calcium-silica-hydrate (C-S-H) gels; calcium carbonate; and hydrated calcium aluminates (Nuclear Decommissioning Authority, 2010b). A significant proportion of the alkali hydroxides/sulfates will dissolve in the initial porewater, and will condition the porewater to a high pH (i.e. >13). As groundwater replaces the initial porewater, the chemistry will be dominated by the dissolution of portlandite, which will maintain the porewater at pH ~12.5 until it is exhausted. After this the pH will be buffered by C-S-H phases with relatively high calcium/silicon molar ratios (Ca/Si) of ~1.5. The incongruent dissolution of C-S-H phases will release calcium and hydroxide ions preferentially, thereby, over time, lowering the Ca/Si ratio and reducing the pH value at which the water is buffered (e.g. Berner, 1988; Harris *et al.*, 2002). The formation of secondary minerals (e.g. calcite, brucite, ettringite, hydrogarnet, CO_3 -hydrotalcite and Al-monocarbonate) may occur due to reactions between the inflowing groundwater, the backfill and the wastes (especially those containing magnesium, sulfur or aluminium). For example, carbonate in groundwater can react with calcium hydroxide from the backfill to form calcite, magnesium in groundwater can react with calcium-rich minerals to form brucite, and calcium and sulfate in groundwater can react with aluminium to form sulfate minerals such as ettringite (Nuclear Decommissioning Authority, 2010b). The secondary minerals could continue to buffer the porewater at pH values of 10 to 12.

Context

Models have been developed previously that predict the long-term ability of a near field to buffer an alkaline pH (e.g. Gould *et al.*, 2001; Heath *et al.*, 2011; Heath and Hunter, 2012). These models represent the effects of both waste and groundwater interactions with the cementitious materials. However, the models are concerned with reactions on the scale of a vault, and not on the scale of a single waste package. Reactive transport models have also been applied to predict pH evolution on the scale of a waste package (Small and Thompson, 2008), and, even more locally, within cracks in the backfill (Swift *et al.*, 2010).

This paper discusses the mineral phases that will probably be present in both the backfill and the encapsulation grouts at times soon after disposal, and proposes a model for the evolution of the cement mineralogy, including the incongruent dissolution of C-S-H gels. The simplified model system was implemented using the program *TOUGHREACT* (Xu *et al.*, 2004), and simulated the spatial and temporal evolution in a GDF over a timescale of 50,000 years. The model includes aqueous speciation, equilibrium chemical reactions and rate-dependent precipitation and dissolution reactions. In addition, the model calculates changes in transport properties (i.e. porosity and permeability) due to precipitation and dissolution reactions and couples the changes in transport properties to the groundwater flow. Thus, effects such as clogging of pores due to the precipitation of secondary minerals are considered.

Numerical Method

System under consideration

The model represents a waste package (a three cubic metre box) as an intact block of encapsulation grout situated towards the upstream boundary of a disposal vault (Fig. 1). Groundwater from the host rock flows into the vault, through about half a metre of backfill, before reaching the upstream surface of the grout. The model is simplified by ignoring the effects of physical containment provided by the steel waste container and the chemistry of its corrosion products, and by ignoring any reactions of the waste itself.

Geometrical model

The grout block and its surrounding backfill were simulated using *TOUGHREACT* (Xu *et al.*, 2004),

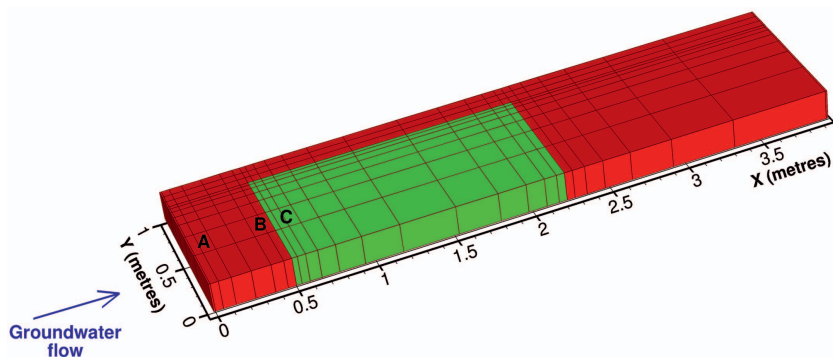


FIG. 1. Schematic representation of 2D model geometry, showing the waste and encapsulation grout inside the three cubic metre box (green) and the surrounding backfill (red). Symmetry considerations require only half of the three cubic metre box to be represented. Groundwater flows into the backfill across the YZ surface. The grid is superimposed, showing refinement of the grid around the three cubic metre box and also at the upstream edge of the backfill. The letters A, B and C refer to the locations of the model predictions presented in Figs 5–7.

a widely used computer code for simulating non-isothermal multi-component reactive geochemical transport. It can be applied to one-, two- or three-dimensional porous and fractured media with physical and chemical heterogeneity. The code can accommodate any number of chemical species present in liquid, gas and solid phases. A variety of equilibrium chemical reactions are considered, such as aqueous complexation, gas dissolution/exsolution, and cation exchange. Mineral dissolution/precipitation can take place subject to either local equilibrium or kinetic controls, with coupling to changes in porosity and permeability (and capillary pressure in unsaturated systems).

A three-dimensional mesh was used to represent the geometry, but the mesh was only one element deep in the z direction, effectively giving a two-dimensional model. Assuming horizontal groundwater flow and vertical symmetry planes (both symmetry planes are aligned with the groundwater flow; one cuts through the mid-point of the waste package, and the other cuts through the backfill halfway between adjacent waste packages), only one half of the grout block was modelled (Fig. 1). The downstream edge of the model was chosen sufficiently far away that it would not affect groundwater flow near the grout block.

The geometry of the model was represented using a grid with 456 elements. A finer grid was used at the interface between the grout and the backfill, and also at the upstream edge of the backfill. Where a finer grid was used, considera-

tion was given to ensure the Courant and von Neumann stability conditions for time step size were satisfied.

Chemical model

The hydration phases present in cementitious materials are likely to evolve and will depend on factors such as the formulation curing time and temperature. Reactions may continue for some time after emplacement of waste in the GDF. As this may have an effect on pH evolution, a literature review was conducted and used to derive starting compositions for backfill and grouts at the time of closure of a GDF.

Backfill composition

The backfill was assumed to be NRVB, formulated from ordinary Portland cement (OPC), hydrated lime (i.e. calcium hydroxide) aggregate, limestone flour and water. Holland and Tearle (2003) have considered the probable hydration phases for various conditions. Using information from that study, and assuming aluminium is partitioned equally between Si-hydrogarnet¹ and Al-monocarbonate¹, led to the backfill composition in Table 1. We avoided using thermodynamic equilibrium to determine

¹ Hydrogarnet is known to be the dominant phase at higher temperatures, such as those likely to occur during curing, but becomes unstable as the temperature falls to 25°C. Al-monocarbonate is expected to be present at lower temperatures (Lothenbach *et al.*, 2008.)

TABLE 1. Initial backfill and grout compositions (volume fraction) and properties.

Mineral	Stoichiometry	Backfill NRVB	Grout		
			3:1 BFS/OPC	9:1 BFS/OPC	3:1 PFA/OPC
Al-ettringite	$\text{Ca}_6\text{Al}_2(\text{SO}_4)_3(\text{OH})_{12}\cdot 26\text{H}_2\text{O}$	0.038	0.029	0.011	0.077
Calcite	CaCO_3	0.178	0.007	0.003	0.011
Al-monocarbonate	$\text{Ca}_4\text{Al}_2(\text{CO}_3)(\text{OH})_{12}\cdot 5\text{H}_2\text{O}$	0.034	—	—	—
Si hydrogarnet	$\text{Ca}_3\text{Al}_2(\text{SiO}_4)_6\cdot 8(\text{OH})_{8,8}$	0.019	—	—	—
C-S-H (Ca/Si = 5.67) [†]	$\text{Ca}_{0,85}\text{Si}_{0,15}\text{O}_{1,15}\cdot 0.85\text{H}_2\text{O}$	0.010	—	—	—
C-S-H (Ca/Si = 4) [†]	$\text{Ca}_{0,80}\text{Si}_{0,20}\text{O}_{1,20}\cdot 0.80\text{H}_2\text{O}$	0.234	—	—	—
C-S-H (Ca/Si = 1.22) [†]	$\text{Ca}_{0,55}\text{Si}_{0,45}\text{O}_{1,45}\cdot 0.55\text{H}_2\text{O}$	—	0.154	—	—
C-S-H (Ca/Si = 1.00) [†]	$\text{Ca}_{0,50}\text{Si}_{0,50}\text{O}_{1,50}\cdot 0.50\text{H}_2\text{O}$	—	0.304	0.093	—
C-S-H (Ca/Si = 0.82) [†]	$\text{Ca}_{0,45}\text{Si}_{0,55}\text{O}_{1,55}\cdot 0.45\text{H}_2\text{O}$	—	—	0.330	0.410
C-S-H (Ca/Si = 0.67) [†]	$\text{Ca}_{0,40}\text{Si}_{0,60}\text{O}_{1,60}\cdot 0.40\text{H}_2\text{O}$	—	—	—	0.113
CO ₃ -hydrotalcite	$\text{Mg}_4\text{Al}_2(\text{OH})_2\text{CO}_3\cdot 3\text{H}_2\text{O}$	—	0.123	0.139	0.043
Al-stratlingite	$\text{Ca}_2\text{Al}_2\text{SiO}_2(\text{OH})_{10}\cdot 3\text{H}_2\text{O}$	—	0.383	0.424	—
Halloysite	$\text{Al}_2\text{Si}_2\text{O}_9\text{H}_4$	—	—	—	0.345
Porosity		0.200	0.200	0.200	0.200
Unreactive volume		0.287			
Permeability (m ²)		1×10^{-16}	1×10^{-18}	1×10^{-18}	1×10^{-18}
Tortuosity		0.15**	0.005***	0.005***	0.005***

[†] In the C-S-H model used, SiO₂, Ca(OH)₂ and calcium silicate hydrate are represented together as members of a set of discrete phases of varying Ca/Si ratio. Those with Ca/Si ratios above ~1.8 are representative of calcium silicate hydrate and the free portlandite present.

* This was calculated from the intrinsic diffusion coefficient of tritiated water, which has been measured to be $6.0 \times 10^{-11} \text{ m}^2 \text{ s}^{-1}$ (Harris and Nickerson, 1995), and the capacity factor, which has been measured to be 0.2. The aqueous molecular diffusion constants are assumed to be $2 \times 10^{-9} \text{ m}^2 \text{ s}^{-1}$.

** A typical intrinsic diffusion coefficient for both sulfate resistant Portland cement and BFS/OPC is about $2.0 \times 10^{-12} \text{ m}^2 \text{ s}^{-1}$ (Harris and Nickerson, 1995).

the composition, because we wanted to include some hydrogarnet which forms at the higher temperatures resulting from the initial hydration reactions. The model then allows the composition to proceed towards equilibrium at rates controlled by the kinetic parameters.

Grout composition

Three grouts were considered: (1) 3 parts blast furnace slag, 1 part ordinary Portland cement (3:1 BFS/OPC); (2) 9 parts blast furnace slag, 1 part ordinary Portland cement (9:1 BFS/OPC); and (3) 3 parts pulverized fly ash, 1 part ordinary Portland cement (3:1 PFA/OPC).

Typical simplified compositions for BFS, PFA and OPC were identified from the literature (Qian *et al.*, 1988; Holland and Tearle, 2003), full details of which are provided in Baston *et al.* (2011). These simplified compositions excluded the alkali elements sodium and potassium as well as iron.

In arriving at the initial composition of the grout it is assumed the waste packages will have been kept in storage for a period of about 100 years following waste encapsulation, and that the water in the grout formulation will be in excess of the amount required to complete all hydration reactions. It was assumed that 100% slag would have reacted by 100 years, but only 90% of the fly ash (to take account of relatively unreactive crystalline phases such as quartz, mullite and hematite).

The hydration phases present in the grouts were calculated assuming a molar volume for each solid phase and that the volume fraction added up to unity. For example, in the case of the two BFS/OPC grouts it was assumed that: (1) ettringite is formed, consuming available SO_3 ; (2) MgO is present as CO_3 -hydrotalcite; (3) the remaining Al_2O_3 is present as Al-stratlingite; and (4) the remaining Ca and Si form C-S-H.

In the case of 3:1 PFA/OPC grout the only difference was to assume that the remaining Al is present in the form of aluminium silicates with a low Al/Si ratio. The choice of minerals was limited to those for which reliable thermodynamic data are available and halloysite, $\text{Al}_2\text{Si}_2\text{O}_5(\text{OH})_4$, was chosen as the best mineral to represent the hydration phases. These assumptions lead to the grout compositions in Table 1; full details are provided in Baston *et al.* (2011).

Solid solution model for C-S-H

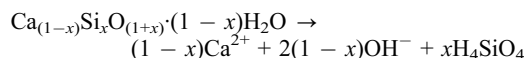
Calcium-silica-hydrate gels are amorphous/nanocrystalline (Allen *et al.*, 2007), metastable,

and exhibit incongruent dissolution with the preferential release of Ca from higher Ca/Si solids. A number of thermodynamic modelling approaches have been proposed based on the representation C-S-H as a solid solution (e.g. Berner, 1988; Kulik and Kersten, 2001; Walker *et al.*, 2007).

Recently, Lichtner and Carey (2006) have presented an approach to incorporating the thermodynamics and kinetics of solid-solution formation into reactive transport models. Their approach represents the continuously variable solid-solution composition by a discrete set of stoichiometric solids and is combined with a kinetic formulation of the rates of reaction. Discretization may be over the entire range of compositions between the end members, or a subset, depending on the system being modelled. An advantage of this algorithm is that modelling solid-solutions is similar to modelling pure mineral phases.

Carey and Lichtner (2007) applied the algorithm to modelling C-S-H as a series of discrete phases described by a binary non-ideal solid solution, with portlandite and amorphous silica as endmembers. Non-ideality of the solid solution was accounted for with a four-term Redlich-Kistler expression. The system was solved using a Lippman phase diagram, fitted to the solubility data of Chen *et al.* (2004). The Lippmann method allows for simultaneous depiction and analysis of solution and solid compositions in terms of a total concentration variable ($\Sigma\Pi$) plotted against the solidus as a mol fraction $\chi_{\text{SiO}_2(\text{am})}$, or the solutus as an activity fraction $\chi_{\text{H}_4\text{SiO}_4}$. The solubility constants of endmember portlandite and $\text{SiO}_2(\text{am})$ were used as fitting parameters and are inconsistent with values in the Nagra/PSI chemical thermodynamic database (Hummel *et al.*, 2002) used for this study. In order to resolve this, data of Chen *et al.* (2004) were refitted (Fig. 2), with the solubility constants of portlandite and $\text{SiO}_2(\text{am})$ weighted to values in the Nagra/PSI database.

Following Carey and Lichtner (2007), the dissolution of C-S-H, written in terms of the mole fraction of SiO_2 (χ) was:



The Lippman variable ($\Sigma\Pi$) is then given by:

$$\log(\Sigma\Pi) = \log\{(a_{\text{Ca}^{2+}})(a_{\text{OH}^-}^2) + a_{\text{SiO}_2}\}$$

For a binary solid solution the excess free energy of mixing ΔG^E , can be modelled by the

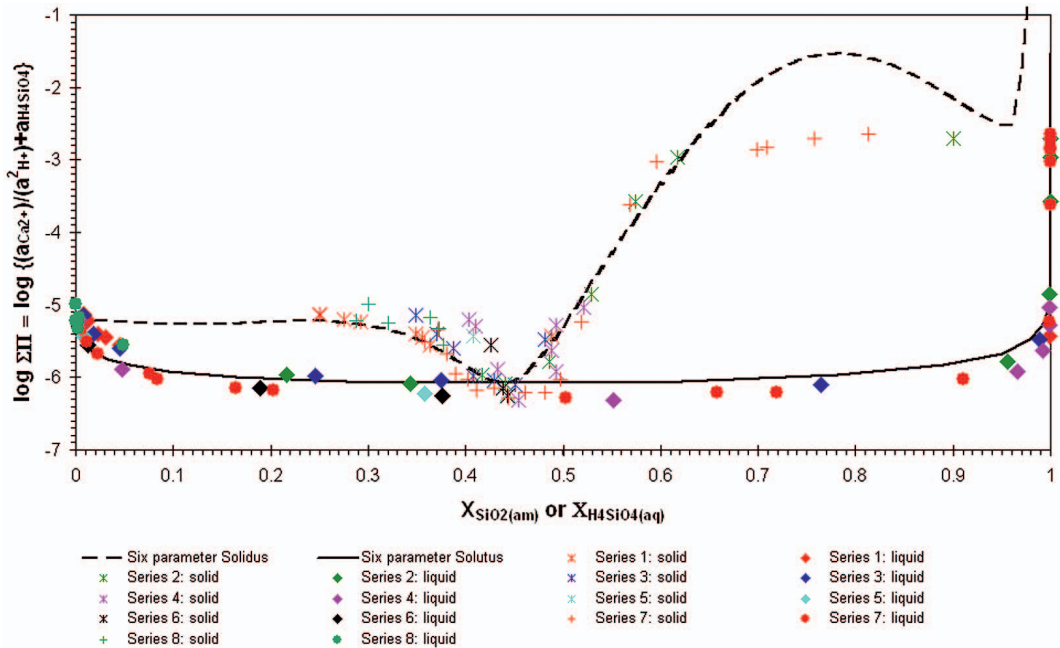
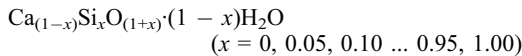


FIG. 2. Our C-S-H model fit to the data of Chen *et al.* (2004) (series 1 to 6). The data of Greenberg and Chang (1965) (series 7 and 8) are also shown. The fitted model parameters were $\log K_{Ca(OH)_2} = -5.199$, $\log K_{SiO_2(am)} = -2.714$, $a_0 = -19$, $a_1 = -2$, $a_2 = 25$, $a_3 = 20$. The minimum where the solid dissolves congruently to a liquid of its own composition and a liquid precipitates a homogeneous solid of the same composition is found at $\chi_{SiO_2(am)}$ of 0.44, with $\log \Sigma \Pi$ of -6.1 . The ordinate, $\Sigma \Pi$, has been written in terms of activity of $H_4SiO_4(aq)$, to be consistent with the Nagra/PSI thermodynamic database. The activity of water is 1.

modified Guggenheim series expansion:

$$\Delta G^E = (\chi_1 \chi_2) RT (a_0 + a_1(\chi_1 - \chi_2) + a_2(\chi_1 - \chi_2)^2 + \dots)$$

where a_0, a_1, a_2, \dots are dimensionless fitting parameters. The values derived were $a_0 = -19$, $a_1 = -2$, $a_2 = 25$, $a_3 = 20$ with the solubility products for portlandite and $SiO_2(am)$ at -5.199 and -2.714 , respectively. These values were used to calculate solubility products for a set of discrete C-S-H phases with the general formula:



using the method of Carey and Lichtner (2007). Thus, values of $x = 0$ and $x = 1$ give the endmembers $Ca(OH)_2$ and SiO_2 respectively. This model allows any Ca/Si ratio to be represented by a combination of adjacent discrete phases in the series. Molar volumes of C-S-H were calculated on the assumption they were proportional to the molar fractions of the endmembers and the excess volume of mixing was zero.

Groundwater composition

Four generic groundwater compositions (Table 2) were chosen for their comprehensiveness and reliability as follows.

(1) ‘Saline’ is illustrated by groundwater sample DET5 from Sellafeld borehole RCF3 (Bond and Tweed, 1995).

(2) ‘High carbonate’ is illustrated by groundwater sample DET6 from Dounreay, and has a high concentration of carbonate (Nirex, 1994).

(3) ‘Low carbonate’ is illustrated by groundwater sample DET8 from Dounreay (Nirex, 1994), and contains the lowest concentration of carbonate. Consequently calcite precipitates at a slower rate, and so the pores in the backfill do not clog.

(4) ‘Clay’ is illustrated by a groundwater from the Callovo-Oxfordian (COX) argillite (Gaucher *et al.*, 2006), and has high concentrations of magnesium and sulfate.

Thermodynamic database

The thermodynamic database used in the modelling was derived as follows. The Nagra/

NEAR FIELD EVOLUTION OF A CEMENTITIOUS REPOSITORY

TABLE 2. Groundwater compositions at 25°C.

	Saline (mol kg ⁻¹)	Highcarbonate (mol kg ⁻¹)	Lowcarbonate (mol kg ⁻¹)	Clay (mol kg ⁻¹)
Na	3.7×10^{-1}	8.4×10^{-3}	8.2×10^{-2}	3.2×10^{-2}
K	4.4×10^{-3}	3.8×10^{-5}	2.5×10^{-4}	7.1×10^{-3}
Mg	5.7×10^{-3}	3.3×10^{-5}	6.8×10^{-4}	1.4×10^{-2}
Ca	2.9×10^{-2}	8.8×10^{-5}	4.8×10^{-2}	1.5×10^{-2}
Sr	2.0×10^{-3}	2.0×10^{-5}	9.9×10^{-4}	1.1×10^{-3}
Al	1.7×10^{-6}	4.6×10^{-7}	5.4×10^{-8}	6.9×10^{-9}
C	1.0×10^{-3}	2.8×10^{-3}	1.6×10^{-4}	3.0×10^{-3}
Si	2.5×10^{-4}	1.1×10^{-4}	7.6×10^{-5}	9.4×10^{-5}
Cl	4.2×10^{-1}	5.3×10^{-3}	1.7×10^{-1}	3.0×10^{-2}
SO ₄ ²⁻	1.2×10^{-2}	2.8×10^{-4}	6.4×10^{-3}	3.4×10^{-2}
pH	7.22	8.75	7.73	7.00

PSI chemical thermodynamic database (Hummel *et al.*, 2002), which has been widely applied to model cement chemistry, was converted to a suitable format for use with *TOUGHREACT*. Next this database was augmented to include hydrolysis reactions for cement phases based on the thermodynamic data given by Lothenbach *et al.* (2006, 2008) and Matschei *et al.* (2007), a subset of the *CEM DATA07 version 07.2* dataset, which excluded the Fe-substituted phases.

Kinetic parameters

In general, the precipitation and dissolution reactions were controlled by kinetic rate expressions based on transition state theory as given in Xu *et al.* (2004). The kinetic parameters are listed in Table 3.

Transport model

The region modelled was specified to be at steady-state initially with a temperature of 25°C. On the faces of the model perpendicular to the *y* axis (Fig.1), the boundary conditions were taken to be closed, because these faces correspond to planes of symmetry. On the other faces of the model, Dirichlet boundary conditions were specified for all of the variables.

With the exception of 'clay' the pressure was specified for all groundwater compositions as being the sum of the hydrostatic pressure and a linear pressure gradient in the *x* direction chosen to give an initial specific discharge of 9×10^{-11} m s⁻¹, appropriate for a fractured, crystalline host rock (Baker *et al.*, 1997). In the case of 'clay', the host rock permeability would be expected to be lower,

and the initial specific discharge was chosen to be 3×10^{-13} m s⁻¹ (Baston *et al.*, 2011).

A total porosity of NRVB of about 0.5 has been measured (Francis *et al.*, 1997) using a combination of mercury intrusion porosimetry (for large pores) and nitrogen desorption (for small pores). However, experiments on the transport of tritiated water through NRVB (Harris and Nickerson, 1995) give a smaller value of about 0.2. This paper applies the latter value because groundwater is more likely to access a similar pore volume to tritiated water, however it is recognized that porosity is a key uncertainty in the modelling study and is discussed later. The model input values for permeability, porosity and tortuosity for backfill and grout are shown in Table 1.

The porosity of the different materials will change due to mineral precipitation/dissolution reactions. The changes in porosity will cause changes in permeability, which were estimated using the Kozeny-Carman relationship (Xu *et al.*, 2004). At each step the changes in permeability are fed back into the simulation and the flows recalculated making this a coupled reactive transport model.

Results

Detailed results are presented for a 2D representation of a three cubic metre box wasteform of 3:1 BFS/OPC grout surrounded by NRVB backfill, through which the 'saline' groundwater percolates.

The predicted spatial evolution of pH, porosity and flow over a 50,000 year timescale is illustrated in Figs 3 and 4. Temporal evolution at three specific locations is illustrated in

TABLE 3. Mineral molar volumes and reaction rates.

Mineral	Formula	Molar volume ($\text{cm}^3 \text{mol}^{-1}$)	Reaction rate ($\text{mol m}^{-2} \text{s}^{-1}$)	Reactive area ($\text{m}^2 \text{g}^{-1}$)	Note
Al-ettringite	$\text{Ca}_6\text{Al}_2(\text{SO}_4)_3(\text{OH})_{12}\cdot 26\text{H}_2\text{O}$	707	1.12×10^{-12}	9.8	(1)
Calcite	CaCO_3	37	1.44×10^{-7}	1	(2)
Al-monocarbonate	$\text{Ca}_4\text{Al}_2(\text{CO}_3)(\text{OH})_{12}\cdot 5\text{H}_2\text{O}$	262	6.31×10^{-12}	5.7	(1)
Si hydrogarnet	$\text{Ca}_3\text{Al}_2(\text{SiO}_4)_{6,8}(\text{OH})_{8,8}$	143	1.12×10^{-12}	10	(3)
Portlandite	$\text{Ca}(\text{OH})_2$	33.226	2.24×10^{-8}	16.5	(2)
C-S-H	—	—	2.75×10^{-12}	41	(1)
SiO_2 (am)	SiO_2	29	—	1	(4)
CO_3 -hydroxalcalite	$\text{Mg}_4\text{Al}_2(\text{OH})_{12}\text{CO}_3\cdot 3\text{H}_2\text{O}$	220	1.12×10^{-12}	10	(3)
Al-stratlingite	$\text{Ca}_2\text{Al}_2\text{SiO}_2(\text{OH})_{10}\cdot 3\text{H}_2\text{O}$	216	1.00×10^{-12}	10	(5)
Halloysite	$\text{Al}_2\text{Si}_2\text{O}_5(\text{OH})_4$	100	1.00×10^{-12}	10	(5)
Brucite	$\text{Mg}(\text{OH})_2$	30	1.00×10^{-7}	1	(6)
Gypsum	CaSO_4	73	1.00×10^{-7}	1	(6)
Monosulfoaluminate	$\text{Ca}_4\text{Al}_2(\text{SO}_4)(\text{OH})_{12}\cdot 6\text{H}_2\text{O}$	309	6.31×10^{-12}	5.7	(1)

(1) These data (i.e. rates and surface areas) are from the doctoral dissertation of Isabel B. Keller (2004) submitted to the Swiss Federal Institute of Technology Zurich. Also, see Baur *et al.* (2004). The molar volume of each discrete C-S-H phase was estimated using $\text{MoleVolumePhase} = x\text{SiO}_2 (\text{MolVolSiO}_2) + x\text{Ca}(\text{OH})_2 (\text{MolVolCa}(\text{OH})_2)$. This simplified approach probably underestimates the density of C-S-H slightly.

(2) See Marty *et al.* (2009) and references therein.

(3) Set similar to ettringite; also see Marty *et al.* (2009).

(4) *TOUGHREACT* includes a kinetic model specifically for $\text{SiO}_2(\text{am})$, which was used in this study.

(5) No data found. Assumed to be similar to ettringite.

(6) Brucite and gypsum were assumed to have reaction rates and surface areas similar to those of calcite.

NEAR FIELD EVOLUTION OF A CEMENTITIOUS REPOSITORY

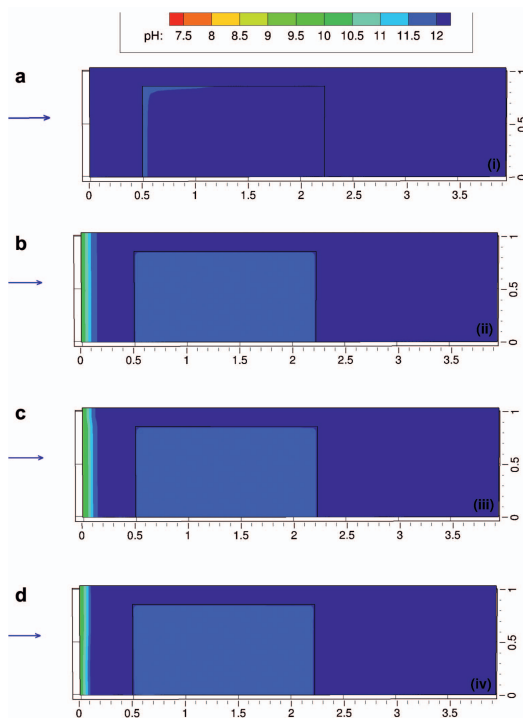


FIG. 3. Predicted evolution of pH at (a) 10 years, (b) 2500 years, (c) 10,000 years and (d) 50,000 years, for groundwater with a ‘saline’ composition flowing through NRVB backfill surrounding a 3:1 BFS/OPC grout. The blue arrow represents the direction of groundwater flow.

Figs 5–7. Initially, the porewater in the backfill is at a pH of 12.4, controlled by the dissolution of portlandite. At the upstream edge there is a decrease in pH with time, due to the removal of portlandite and C-S-H, primarily by their dissolution in the inflowing groundwater or their reaction with carbonate to form calcite (carbonation). After 2500 years no significant change in pH is observed and the pH remains at a value of approximately 9.9. The reason for this behaviour is a decrease in the porosity of the region (Fig. 4) causing a decrease in flow and a reduction in the interaction between the groundwater and the backfill. At 30,000 years the backfill becomes effectively sealed by a layer of calcite at the upstream face (Fig. 5). The carbonation of cement surfaces is well-documented (Cowie and Glasser, 1992; Harris *et al.*, 2003) and so, in this respect, the model predictions agree with experimental observations. In addition to calcite, the formation

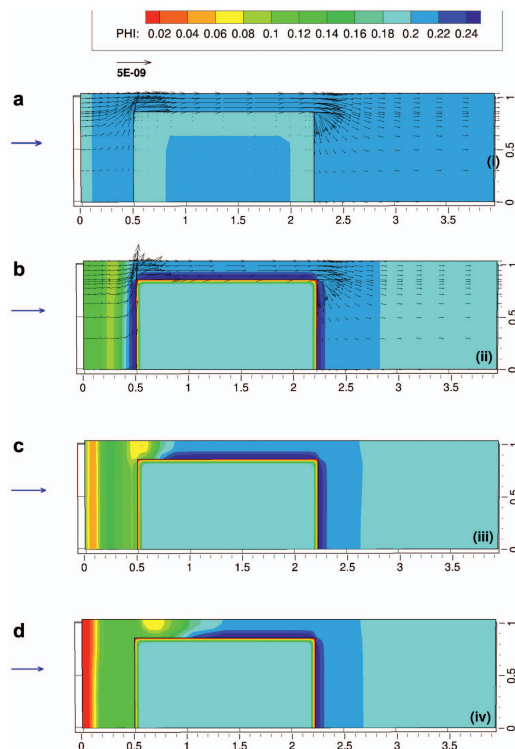


FIG. 4. Predicted evolution of porosity (PHI) and flow at (a) 10 years, (b) 2500 years, (c) 10,000 years and (d) 50,000 years, for groundwater with a ‘saline’ composition flowing through NRVB backfill surrounding a 3:1 BFS/OPC grout. The blue arrow represents the direction of groundwater flow. The length of the flow vectors corresponds to the magnitude and direction of flow, with the legend showing a flow arrow corresponding to $5 \times 10^{-9} \text{ m s}^{-1}$. The flow vectors at 10,000 years and at 50,000 years cannot be seen because the flow is very low.

of some CO_3 -hydrotalcite is predicted. Brucite and gypsum form at early times, but their volume fractions decrease after about 2500 years, which coincides with a drop in the pH due to dissolution of all C-S-H in a narrow region of width 0.15m at the upstream face. Because the grout has a lower permeability than the backfill, groundwater tends to be channelled through the backfill around the grout block (Fig. 4).

The bulk of the backfill remains buffered at the original pH of 12.4 over the 50,000 year timescale and the porewater composition is relatively stable because groundwater flow is reduced to negligible levels.

A: In the backfill (at the inflow boundary)

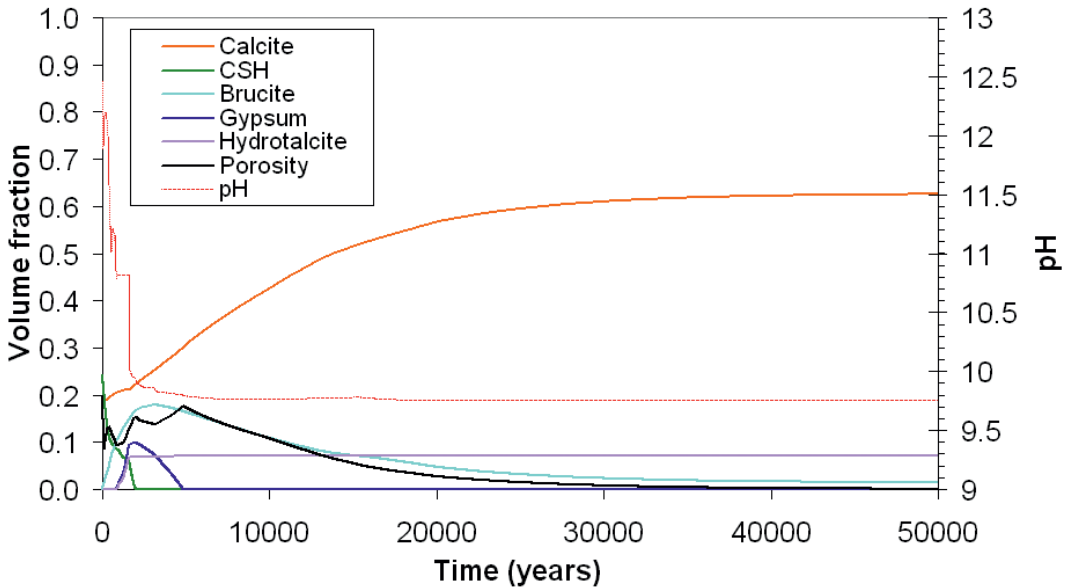


FIG. 5. Predicted evolution in the backfill (at the inflow boundary) of the pH, porosity and volume fraction of solid phases, over a period of 50,000 years, for groundwater with a 'saline' composition flowing through backfill surrounding a 3:1 BFS/OPC grout; (at location A as shown on Fig. 1). The volume fractions of the solid phases plus the porosity add up to unity.

B: In the backfill (at the interface with grout)

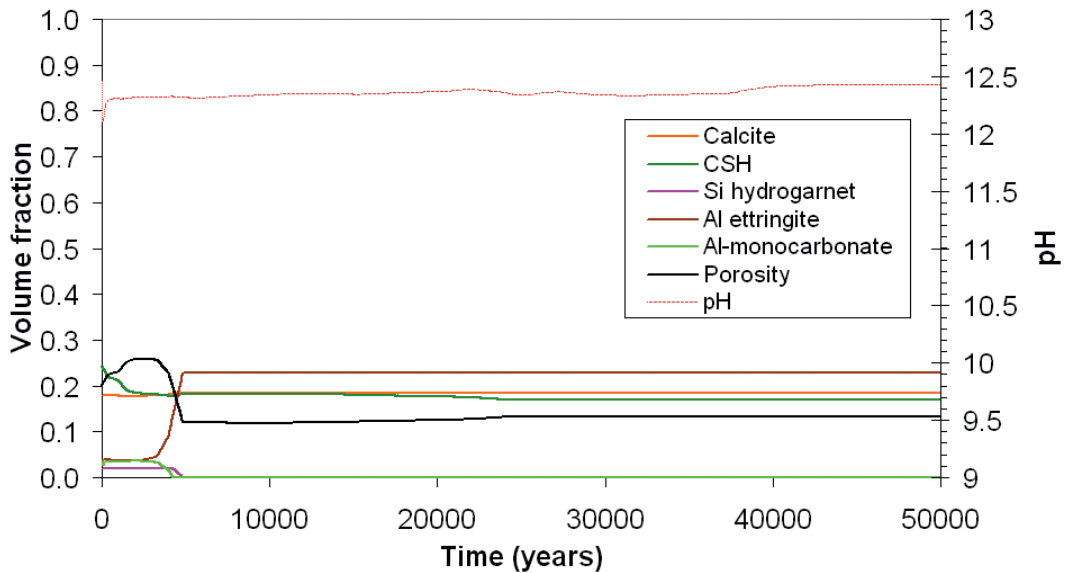


FIG. 6. Predicted evolution in the backfill (at the interface with the grout) of the pH, porosity and volume fraction of solid phases, over a period of 50,000 years, for groundwater with a 'saline' composition flowing through backfill surrounding a 3:1 BFS/OPC grout; (at location B as shown on Fig. 1).

C: In the grout (at the interface with backfill)

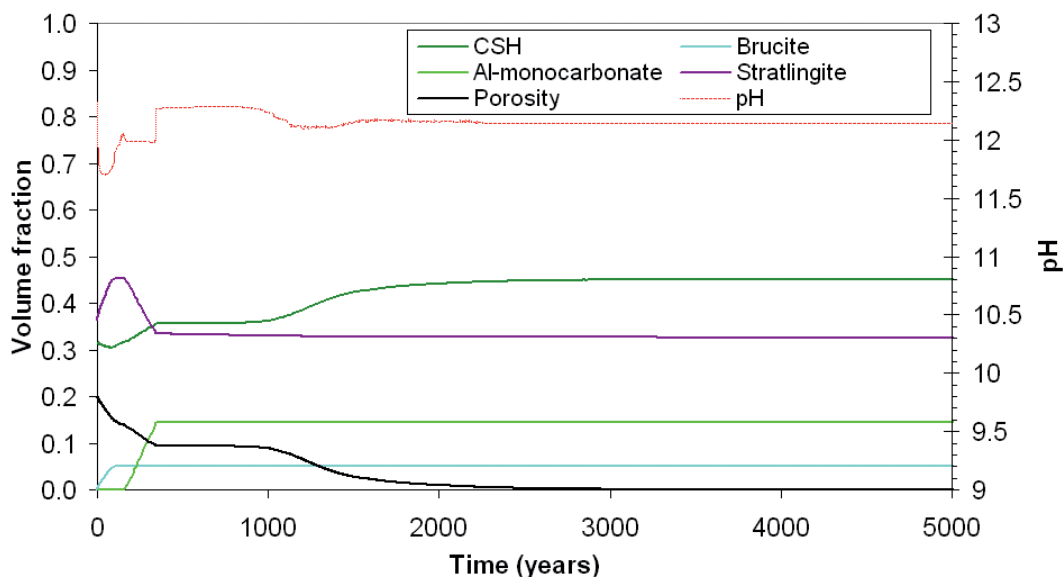


FIG. 7. Predicted evolution in the grout (at the interface with the backfill) of the pH, porosity and volume fraction of solid phases, over a period of 50,000 years, for groundwater with a 'saline' composition flowing through backfill surrounding a 3:1 BFS/OPC grout; (at location C as shown on Fig. 1).

The other region where there are significant mineral changes, with a corresponding decrease in porosity, is close to the interface between the grout and the backfill. In the grout, Al-monocarbonate and C-S-H form as calcium in the backfill porewater diffuses into the grout. In the backfill, Al-ettringite forms as aluminium diffuses from the grout into the backfill. The pH of the grout is slightly below that of NRVB, because the higher silica and alumina content of the formulation means there is no free portlandite after hydration. The bulk of the grout remains stable at its initial value of pH 12 over 50,000 years due to its low permeability and the mineral reactions that cause pore clogging at the surface of the grout and reduce groundwater inflow.

Other scenarios using different groundwaters and alternative grout compositions have also been investigated and are detailed in the project report (Baston *et al.*, 2011). These scenarios showed dissolution/precipitation reactions occurring at the upstream edge to be strongly dependant on the chemical composition of the inflowing groundwater. For example, although calcite forms for the 'low carbonate' groundwater, it is not precipitated in sufficient quantity to fill the porosity over a

period of 50,000 years. In the case of the 'clay' groundwater, significant quantities of brucite and gypsum form in addition to calcite.

Discussion

The models and conclusions are based upon several simplifying assumptions that have been required to undertake the modelling. Equally there is a range of uncertainties in the model and its data, which mean that caution is needed when interpreting the results for the evolution of pH in the GDF. For example, the model relies on some experimental data and there are inherent difficulties in upscaling from relatively short duration and small scale laboratory experiments to a model that attempts to consider large dimensions and long time periods.

However, the key uncertainties in the model predictions relate to the formation of secondary minerals (notably calcite) that limit the extent of groundwater flow and therefore maintain the high pH within the grout over long timescales. As a result, subsequent work was carried out, described in the project report (Baston *et al.*, 2011), to investigate the sensitivity of the model to

(1) changes in initial porosity of the NRVB; (2) a refinement of the C-S-H solid solution model and a review of molar volumes of solid phases; and (3) the inclusion of a host rock. These uncertainties, along with other assumptions are discussed below.

The choice of porosity of the NRVB is a key uncertainty in the modelling. Notably, the initial porosity of NRVB was taken to be 0.2, which corresponds with experiments that use tritiated water to calculate the porosity of NRVB (Harris and Nickerson, 1995). However, a widely quoted total porosity value for NRVB is 0.5 (e.g. Nuclear Decommissioning Authority, 2010b). Clearly the evolution of the porosity has an important effect on the maintenance of pH and fluid flow through the system. Baston *et al.* (2011) carry out subsequent calculations that apply a total porosity of 0.5 for NRVB and include a hard host rock. However, the predicted mineral reactions and pH evolution are very similar to the original scenario that considers a porosity of 0.2 for NRVB because the dominant factor controlling the predicted behaviour is mineral precipitation in the fracture porosity of the host rock which significantly reduces groundwater flow through the vault. The porosity of the host rock is much lower than that of the NRVB and therefore a small amount of mineral precipitation in the host rock is sufficient to cause a significant reduction in the groundwater flowing through the vault. Because the flow is restricted in this way, the NRVB at the inflow is exposed to a lower volume of groundwater and therefore its solid phase composition and pH remains stable with time. The bulk of the NRVB and grout is predicted to remain above pH 12 for the duration of the calculation. For a clay host rock scenario, a similarly stable solid phase and pH evolution scenario is predicted.

The formation of calcite in cementitious materials which have been exposed to carbonate has been observed in experimental studies, and so is likely to occur in the GDF. The model assumes a simple Kozeny–Carman expression to relate changes in permeability to changes in porosity. The predicted timescale for calcite to clog the pores in the backfill depends on this assumption, and therefore is uncertain. The situation may be further complicated by the possibility that a significant proportion of the groundwater may flow preferentially through cracks (e.g. in the backfill around waste packages; Swift *et al.*, 2012).

Later calculations described in Baston *et al.* (2011) updated the solid solution model fit of the

Lippmann phase diagram by applying a regression analysis to the experimental datasets of Chen *et al.* (2004) and Greenberg and Chang (1965). The improved Lippmann model parameters were $\log K_{\text{Ca}(\text{OH})_2} = -5.199$, $\log K_{\text{SiO}_2(\text{am})} = -2.714$, $a_0 = -19.4926$, $a_1 = -2.5962$, $a_2 = 21.2213$, $a_3 = 5.4133$. The solidus fit was much improved at $\chi_{\text{SiO}_2} > 0.6$. In addition, the number of discrete C-S-H phases was increased from 20 to 100 which provided a smoother transition between discrete phases, and solubility constants for the discrete phases were recalculated based on the updated Lippmann variable. The updated C-S-H model was verified using the equilibration of C-S-H with water and the predicted aqueous pH, calcium and silicon concentrations were compared with experimental data from Chen *et al.* (2004) and Harris *et al.* (2003). An improved fit was noted for the prediction of aqueous silicon concentration, while the predictions of pH and calcium concentration remained similar.

A comparison of cement phase density values from Balonis and Glasser (2009) against those applied in the original scenario was carried out in a second phase of work described by Baston *et al.* (2011); the two datasets were generally found to be in good agreement. In addition, the values for the molar volumes of C-S-H phases with varying Ca/Si ratios were reassessed. The refinement of the C-S-H solid solution model fit and molar volumes made no appreciable difference to the model predictions carried out in the second phase of work (Baston *et al.* 2011).

Subsequent calculations reported by Baston *et al.* (2011) examine the effect of including a ‘hard rock’ or ‘clay’ host rock. These calculations show that for hard rock, the high pH, calcium-rich porewaters diffuse into the rock, causing calcite precipitation which reduces the host rock’s porosity. As a result, the porosity of the host rock is predicted to block flow into the NRVB, before the porosity of the NRVB itself becomes fully blocked. Similarly, if a clay host rock is included, the formation of the secondary minerals in the clay is predicted to block the porosity, and prevent flow into the NRVB before the porosity of the NRVB itself becomes fully blocked.

The model assumes that the metal container is not present. In the short term, the container would be expected to act as part of a multi-barrier system to contain the waste and isolate or delay advective transport of the inflowing groundwater until such time as it has fully or partially corroded. During the period when the container

is fully intact, any influx of groundwater would be limited to that able to diffuse into the waste via the small vent in the container that is designed to allow the release of gas. The corrosion of the steel container will generate corrosion products such as magnetite or other iron oxide or oxyhydroxide phases which may interact with the cement mineralogy and pH, but these effects have not been modelled. Instead, the model assumes full interaction between the NRVB and backfill from the initial time; this would not be expected to occur in practice.

The model also neglects any effects of the wastes. For example, corrosion of reactive metals and degradation of organic materials contained within the wastes could reduce the pH conditions around individual waste packages, and produce gas such as carbon dioxide and methane. Equally, the reactions between the wastes and NRVB have been neglected. For example, NRVB containing portlandite may be expected to readily react with aluminium, sulfur, iron and carbonate from the wastes (and groundwater) which may result in solid phases such as monosulfate and ettringite.

The choice of model input parameters have uncertainties. In particular, there is some uncertainty in the most probable solid phases formed in high alumina grouts such as 3:1 PFA/OPC. Applying the approach used in calculating the BFS/OPC phase compositions yielded a mix in which all Ca is present as stratingite with none as C-S-H. It was thought that a more likely distribution for this grout would be the formation of aluminium silicates with a higher Si/Al ratio, but the choice of solid phases was limited to those for which reliable thermodynamic data was available and halloysite was chosen as the best approximation to represent them. Although not ideal, this was a compromise as it is recognized that halloysite is a hydrated kaolin-like clay mineral, more typically found in weathered soils.

The kinetic reaction rates of the solid phases (Table 3) showed that calcite has a relatively fast reaction rate (with brucite and gypsum assigned similar values). Given that one of the key parameters in the modelling is the precipitation of calcite to reduce fluid flow, it could be expected that any uncertainty in the reaction rate of calcite will have a corresponding effect on the timescale of the changes occurring in the model. The remaining solid phases have much slower kinetic reaction rates and therefore the model results are expected to be less sensitive to changes in their rates.

The reactions at the interface between the backfill and the grouts are also uncertain. Although predicted by thermodynamic modelling, some of the reactions have not been observed experimentally (such as formation of carbonate within the grout). However, if the grouts do react with the backfill to form a lower permeability coating, the release of radionuclides from the wasteform could be reduced significantly.

Summary

A model has been developed to describe the interactions between the cementitious backfill in a geological disposal facility for radioactive waste, different grout formulations and various groundwater compositions.

Detailed results are presented only for a 2D representation of a three cubic metre box wasteform of 3:1 BFS/OPC grout surrounded by NRVB, through which 'saline' groundwater percolates. The model predicts a reduction in the backfill porosity due to dissolution of portlandite and C-S-H and the formation of calcite, particularly at the upstream edge of the vault. The mineral reactions seal the backfill, preventing further ingress of groundwater, which results in a pH >12 being maintained thereafter in the bulk of the backfill.

The model also predicts a reduction in porosity of the grout close to the backfill interface primarily due to the formation of C-S-H and Al-monocarbonate. This isolates the grouts from the backfill, so that the pH within the grouts is unchanged over an extended period.

Other model examples show similar effects in most cases (Baston *et al.*, 2011). In particular, the degree of reduction in backfill porosity, particularly at the upstream edge of the vault depends on the groundwater composition.

The effect of reduced porosity and permeability, particularly at the upstream edge of the vault has implications for the wider context of geological disposal. For example, the design features of the NRVB backfill are to have a high porosity to facilitate sorption, maintain uniform chemical conditions throughout a GDF and allow the release of gas generated from the waste (Nuclear Decommissioning Authority, 2010b). In most cases the results of this study predict sealing and isolation of the backfill which presents a problem that contradicts its stated design. However, the calculations show that reduced porosity is confined to a limited volume of the

upstream edge of the vault, which may imply that the bulk of the NRVB remains unaffected and able to maintain its useful chemical barrier properties. Clearly further investigation is needed.

Key model uncertainties of the porosity of NRVB, the C-S-H model and the impact of the host rock have been examined in subsequent modelling along with a discussion of other model uncertainties and assumptions. There is some uncertainty about whether the reactions that are assumed to occur at the interface between the grouts and the backfill are correct since they have not been observed experimentally; further investigation is needed to validate this aspect of the model. Equally, the predicted timescale for calcite to clog the pores in the backfill is uncertain as it depends on the model treatment of porosity. Despite these reservations, the model provides a useful basis for developing a conceptual understanding of the spatial and temporal evolution within a cement-based engineered barrier system of a GDF.

Acknowledgements

This work was funded by the United Kingdom's Nuclear Decommissioning Authority.

References

- Allen, A.J., Thomas, J.J. and Jennings, H.M. (2007) Composition and density of nanoscale calcium-silicate-hydrate in cement. *Nature Materials*, **6**, 311–316.
- Baker, A.J., Chambers, A.V., Jackson, C.P., Porter, J.D., Sinclair, J.E., Sumner, P.J., Thorne, M.C. and Watson, S.P. (1997) *Nirex 97. An Assessment of the Post-closure Performance of a Deep Waste Repository at Sellafield. Volume 3: the Groundwater Pathway*. Nirex, Science Report S/97/012.*
- Balonis, M. and Glasser, F.P. (2009) The density of cement phases. *Cement and Concrete Research*, **39**, 733–739.
- Baston, G.M.N., Glasser, F.P., Smith, V. and Hoch, A.R. (2011) *Modelling pH evolution in the near-field of a geological disposal facility for ILW/LLW*. Serco Report SERCO/003011/002b Issue 2b.*
- Baur, I., Keler, P., Mavrocordatos, D., Wehrli B. and Johnson, C.A. (2004) Dissolution-precipitation behaviour of ettringite, monosulfate, and calcium silicate hydrate. *Cement and Concrete Research*, **34**, 341–348.
- Berner, U.R. (1988) Modelling the incongruent dissolution of hydrated cement minerals. *Radiochimica Acta*, **44/55**, 387–393.
- Bond, K.A. and Tweed, C.J. (1995) *Groundwater Compositions for the Borrowdale Volcanics Group, Boreholes 2, 4 and RCF3, Sellafield, Evaluated using Thermodynamic Modelling*. Nirex Report NSS/R397.*
- Carey, J.W. and Lichtner P.C. (2007) Calcium silicate hydrate (C-S-H) solid solution model applied to cement degradation using the continuum reactive transport model FLOTRAN. Pp. 73-106 in: *Transport Properties and Concrete Quality: Materials Science of Concrete* (B. Mobasher and J. Skalny, editors) American Ceramic Society Special Volume. John Wiley and Sons, New Jersey, USA.
- Chen, J.J., Thomas, J.J., Taylor, H.F.W and Jennings, H.M. (2004) Solubility and structure of calcium silicate hydrate. *Cement and Concrete Research*, **34**, 1499–1519.
- Cowie, J. and Glasser, F.P. (1992) The reaction between cement and natural waters containing dissolved carbon dioxide. *Advances in Cement Research*, **4**, 119–134.
- Francis, A.J., Cather, R. and Crossland, I.G. (1997) *Nirex Safety Assessment Research Programme: Development of the Nirex Reference Vault Backfill*. Nirex Report S/97/014.*
- Gaucher, E.C., Blanc, P., Bardot, F., Braibant, G., Buschaert, S., Crouzet, C., Gautier, A., Girard, J., Jacqout, E., Lassin, A., Negrel, G., Tournassat, C., Vinsot, A. and Altmann, S. (2006) Modelling the porewater chemistry of the Callovian–Oxfordian formation at a regional scale. *Comptes Rendus Geoscience*, **338**, 917–930.
- Gould, L.J., Harris, A.W. and Haworth, A. (2001) *Calculation of the Volume of Backfill Required in the Near-field of a Repository*. AEA Technology Report AEAT/ERRA-2270.*
- Greenberg, S.A. and Chang, T.N. (1965) Investigation of colloidal hydrated calcium silicates: ii. Solubility relationships in the calcium oxide/silica–water system at 25°C. *Journal of Physical Chemistry*, **69**, 182–188.
- Harris, A.W. and Nickerson, A.K. (1995) *The Mass-transport Properties of Cementitious Materials for Radioactive Waste Repository Construction*. Nirex Report NSS/R309.*
- Harris, A.W., Manning, M.C., Tearle W.M. and Tweed, C.J. (2002) Testing of models of the dissolution of cements—leaching of synthetic C-S-H gels. *Cement and Concrete Research*, **32**, 731–746.
- Harris, A.W., Manning, M.C. and Tearle, W.M. (2003) *Carbonation of Nirex Reference Backfill*. Serco Report SERCO/ERRA-0454.*
- Heath, T.G. and Hunter, F.M.I. (2012) *Calculation of Near-field pH buffering: Effect of Polymer Encapsulant*. Serco Report SA/ENV-0909 Issue 2.*

- Heath, T.G., Hunter, F.M.I., Magalhaes, S. and Smith, V. (2011) *Spreadsheet Model for the Impact of Waste Packages on Local pH Conditioning*. Serco Report SERCO/TAS/000356/01 Issue 1.*
- Holland, T.R. and Tearle, W.M. (2003) *A Review of NRVB Mineralogy*. Serco Report SERCO/ERRA-0455.*
- Hummel, W., Berner, U., Curti, E., Pearson, F.J. and Thoenen, T. (2002) *Nagra/PSI Chemical Thermodynamic Data Base 01/01*. Nagra Report NTB 02-16. Nagra, Wettingen, Switzerland.
- Kulik, D.A. and Kersten, M. (2001) Aqueous solubility diagrams for cementitious waste stabilization systems: II, End-member-stoichiometries of ideal calcium silicate hydrate solid solutions. *Journal of the American Ceramic Society*, **84**, 3017–3026.
- Lichtner, P.C. and Carey, J.W. (2006) Incorporating solid solutions in reactive transport equations using a discrete-composition approach. *Geochimica et Cosmochimica Acta*, **70**, 1356–1378.
- Lothenbach, B. and Winnefeld, F. (2006) Thermodynamic modelling of the hydration of Portland cement. *Cement and Concrete Research*, **36**, 209–226.
- Lothenbach, B., Matschei, T., Möschner, G. and Glasser, F.P. (2008) Thermodynamic modelling of the effect of temperature on the hydration and porosity of Portland cement. *Cement and Concrete Research*, **38**, 1–18.
- Marty, N.C.M., Tournassat, C., Burnol, A., Giffaut, E. and Gaucher, E.C. (2009) Influence of reaction kinetics and mesh refinement on the numerical modelling of concrete/clay interactions. *Journal of Hydrology*, **364**, 58–72.
- Matschei, T., Lothenbach, B. and Glasser, F.P. (2007) Thermodynamic properties of Portland cement hydrates in the system CaO–Al₂O₃–SiO₂–CaSO₄–CaCO₃–H₂O. *Cement and Concrete Research*, **37**, 1379–1410.
- Nirex (1994) *Downreay Geological Investigations: Hydrogeology*. Nirex Report 660.*
- Nuclear Decommissioning Authority (2010a) *Geological Disposal: Radionuclide Behaviour Status Report*. NDA Report NDA/RWMD/034.*
- Nuclear Decommissioning Authority (2010b) *Geological Disposal: Near-field Evolution Status Report*. NDA Report NDA/RWMD/033.*
- Qian, J.C., Lachowski, E.E. and Glasser, F.P. (1988) Microstructure and chemical variation in class F fly ash glass. *Materials Research Society Symposium Proceedings*, **113**, 45–53.
- Small, J.S. and Thompson, O.R. (2008) *Development of a Model of the Spatial and Temporal Evolution of pH in Cementitious Backfill of a Geological Repository*. National Nuclear Laboratory Report NNL(08) 9601 Issue 4.
- Swift, B.T., Bamforth, P.B., Hoch, A.R., Jackson, C.P., Roberts, D.A. and Baston, G.M.N. (2010) *Cracking, Flow and Chemistry in NRVB*. Serco Report SERCO/TAS/000505/01 Issue 2.*
- Swift, B.T., Bamforth, P.B. and Baston, G.M.N. (2012) Cracking in a cementitious backfill, and the implications for flow and chemistry. *Mineralogical Magazine*, **76**, 3071–3082.
- Walker, C.S., Savage, D., Tyrer, M. and Vala Ragnarsdottir, K. (2007) Non-ideal solid solution aqueous solution modeling of synthetic calcium silicon hydrate. *Cement and Concrete Research*, **37**, 502–511.
- Xu, T., Sonnenthal, E., Spycher, N. and Pruess, K. (2004) *TOUGHREACT User's Guide: A Simulation Program for Non-isothermal Multiphase Reactive Geochemical Transport in Variably Saturated Geologic Media*. Lawrence Berkeley National Laboratory Report LBNL-55460. Lawrence Berkeley National Laboratory, Berkeley, California, USA.

* Available at <http://www.nda.gov.uk>